



Preliminary laboratory assessment for lignocellulosic biomass drying

Evaluación preliminar de laboratorio para el secado de biomasa lignocelulósica

Julio F. Mata-Segreda

<https://orcid.org/0000-0002-2356-4699>

Biomass Laboratory, School of Chemistry, University of Costa Rica, 11501-2060, Costa Rica

Autor correspondiente: julio.mata@ucr.ac.cr

Enviado: 2 de Agosto de 2025. **Aceptado:** 1 de octubre de 2025

<https://doi.org/10.59722/rcvn.v3i2.993>

Abstract

The drying of lignocellulosic biomasses is an important unit operation in regions with agro-industrial economies and circular economy activities in general. The procedures used in the author's laboratory to obtain drying kinetic data, and their mathematical processing are discussed, to quantify the characteristics of lignocellulosic biomasses and porous materials in general. The results serve as a starting point for the design and operation of industrial dryers.

Keywords

Drying kinetics, dynamic porosity, minimal energy drying cost, molecular diffusion in pores.

Resumen

El secado de biomasa lignocelulósica es una operación unitaria de importancia en regiones con economías agroindustriales y actividades propias de economía circular en general. Se discuten los procedimientos usados en el laboratorio del autor para la obtención de datos cinéticos de secado y su tratamiento matemático, para cuantificar las características de biomasa lignocelulósica y materiales porosos en general. Los resultados son el punto de partida para el diseño y operación de secadores industriales.

Palabras clave

Cinética de secado, costo energético mínimo de secado, difusión molecular en poros, porosidad dinámica.



Introduction

Drying of lignocellulosic biomasses and other agro-industrial residues is an area of direct interest in regions with agro-industrial economies. The reduction of moisture is a first physical treatment on raw materials, before any extraction or physical/chemical change is conducted.

Reduction of water content (or other liquids) from porous materials is a common technological operation. The theoretical aspects of this unit operation apply to different areas such as food preservation by moisture reduction (Inyang, et al., 2018), heterogeneous catalysis (Fernández-Solano & Mata-Segreda, 2021) or performance of building materials (Carter and Kibler, 1978; Mora et al., 2019).

The design, construction and operation of industrial dryers must be consistent with prior observations on the drying kinetic behaviour of specific porous materials at laboratory level. These previous experiments are necessarily done, for the assessment of the ease of moisture reduction of porous materials.

Most published papers on material drying deal with specific cases, and fewer papers deal with the theoretical aspects of diffusion of fluids in pores (Yiotis, et al., 2006; Songgok, et al. 2012; Inyang, et al., 2018; Alcántara, et al., 2024; Schlaich, et al., 2025) or basic mathematical analysis of drying kinetics data (Smirnov & Lysenko, 1989; Kemp, et al., 2001; Mora, et al., 2019). Some mathematical proposals have no direct bearing on molecular conceptions of the drying process but rely more on goodness-of-fit criteria.

This work gives the simpler view of the macro- and microscopic aspects of drying studies at our laboratory, than the more complex versions presented in unit-operations textbooks and review articles (Geankoplis, 2006; Cai, et al., 2023; Schlaig, et al., 2025). This work is not intended to be a review article, but a document that shares our experience on the subject, specially aiming at the needs of laboratories of small companies. It should not be expected to deal with the drying of specific materials, either. Therefore, no considerations will be made for the effect of the variables necessary for optimal reduction of moisture such as environmental humidity, temperature, or velocity of purging air currents.

Working model

Drying dynamics is influenced by mass and heat transfer, as well as diffusion of fluid from the moist sample into the surrounding aerial phase (Geankoplis, 2006). The operation is conducted in industrial systems under the flow of a purge gas, to enhance water recovery and reduce drying times and energy.

In our model, the molecular picture of drying of porous materials is a process that initially involves the direct phase transfer from the liquid film on the particles surface to a stagnant surrounding aerial space. It is observed that the drying rate during this stage is constant. It is interpreted that this zero-order kinetic regime occurs if the rate of evaporation equals the rate of arrival of evaporating molecules at the solid-gas interface. This mechanistic proposal is like the situation of pure liquids, and implies an almost constant interfacial composition with a constant vapour pressure; as indicated by the traditional Hertz-Knudsen equation (Mata-Segreda, 2025):

$$\frac{-dn_{liq}/dt}{\text{Fluxional area}} = \kappa \frac{p_v(T)}{\sqrt{2\pi MRT}} \quad (1)$$

where κ is the so-called condensation factor, $p_v(T)$ is the liquid vapour pressure at temperature T , M is the liquid molecular mass, and RT has the usual meaning. The rate of evaporation is clearly constant at a fixed temperature.

As the drying process occurs, “dry islands” appear on the solid matrix surface once a critical degree of drying $[x_c]$ is reached, and the kinetics is no longer zero order. The hydraulic continuity between bulk moist material and particle surface no longer exists. From this point afterwards, the kinetics is determined by mass transfer through the solid matrix pores. As said above, the zero-order regime extends for as long as H_2O molecules arrive at the particle-air interface as fast as evaporation occurs. It then follows that those materials with higher x_c (longer constant-rate intervals) match those with high mass-transfer characteristics (Puente-Urbina, et al. 2016).



This second rate-decreasing stage is the result of:

- a) slower liquid mobility inside the matrix pores, thus reducing the probability of transfer to the near aerial phase,
- b) the fluxional areas of liquids soaking porous materials are also diminished, and
- c) liquid desorption from porous materials requires the breaking apart of any stabilising interactions of the imbibing fluid with the pore walls. All three conditions make overall evaporation more difficult than the case of a free liquid surface.

For this rate-decreasing stage, it is intuitively certain that the drying rate of a particular material at temperature T and through a certain fluxional area must be proportional to the residual moisture content. This mathematical assertion is stated as:

$$\text{Drying rate} \propto \text{Residual moisture} \quad (2)$$

Materials and Methods

Kinetic drying measurements are usually conducted in our laboratory at 50 °C and the normal atmospheric pressure over the University of Costa Rica central campus [(87 ± 2) kPa at 1229 m above sea level]. The relative humidity in the laboratory is maintained at around 65 %.

Our methodology uses drying balances and the absence of purging air currents. These balances have draft shields that allow doing gravimetric measurements under a minimum effect from surrounding air drafts in the laboratory environment. These instruments are also built with heat shields that allow samples to be heated quite evenly at the experimental temperature. Construction details are provided by manufacturers. The kinetic measurements are done by following the mass loss of a sample, as a function of time at constant temperature.

The solid samples are typically soaked overnight with distilled water. Before the gravimetric measurements are conducted, the materials are filtered (Büchner funnel) and gently pressed between kitchen towels, to obtain a free-flowing solid. One crucial point is to keep samples under refrigeration in tightly stoppered containers prior to kinetic measurements,

to avoid inadvertent moisture loss.

The biomass sample (~ 10 g) is then loosely spread on the balance aluminium dishes, and the mass – time data monitored until no further change occurs, a point in time indicated by the drying balance.

Results

Figure 1 shows a typical drying result of a sample of compost made from coffee dregs, as a model material like common lignocellulosic biomasses. In this run, the drying operation time profile shows an initial linear decay, followed by a rate-decreasing kinetic phase. The data of the experiment shown indicate that thermal equilibration between the specimen and sample chamber takes ~3 minutes. The linear range extends from 3,0 min up to 35,0 min ($r_p = 0,9995$).

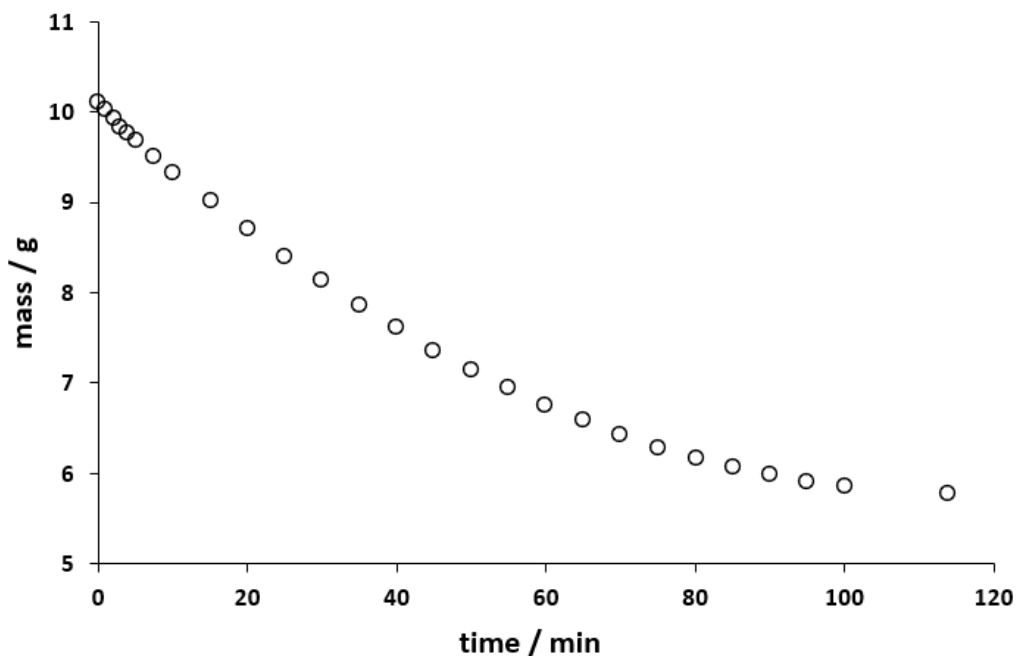


Figure 1. Typical mass-time data at 50 °C and 87 kPa, for drying of a compost made from industrial coffee dregs.

The initial sample of mass $m_{initial} = 10,101$ g dries down to a final mass $m_{final} = 5,777$ g. The total H₂O desorption was 42,8 % of the initial sample mass. The ease of drying of porous

materials depends on three characteristics of the different solid matrices:

- a) volumetric porosity (fraction of total volume that equals empty space),
- b) pore constrictivity (pore dimensions), and
- c) pore tortuosity (mean trajectory inside pores, relative to macroscopic particle dimensions).

We have termed these three characteristics together as *dynamic porosity* (Puente-Urbina, et al., 2016; Conejo-Barboza and Mata-Segreda, 2018). For a particular sample, we usually perform three runs, or five, depending on the reproducibility obtained.

The kinetic description of the entire drying processes is described by the so-called Krischer plot, which gives the rate of drying as a function of residual moisture, as shown in figure 2 (Kemp, et al., 2001). The dynamics of drying shows the initial constant-rate kinetic phase, that is, mass loss decreases at a constant rate during this period ($-dm/dt = \text{constant}$). Our experience dictates that the initial mass-time linear relationship is described with a Pearson's $|r_p| \geq 0,9995$ (99,9 % goodness of fit). The system eventually achieves a critical degree of drying $[x_c]$, where $-dm/dt$ becomes discontinuous, though $m = m(t)$ is a continuous function.

The usual way to describe the data is by using the extent of drying (x) as the dependent variable. It is clearly defined as:

$$x(t) = \frac{m_{\text{initial}} - m(t)}{m_{\text{initial}} - m_{\text{final}}} \quad (3)$$

The rate of advancement of the drying operation is then:

$$\frac{dx}{dt} = \frac{(-dm/dt)}{(m_{\text{initial}} - m_{\text{final}})} \quad (4)$$

Figure 2 shows the concept.

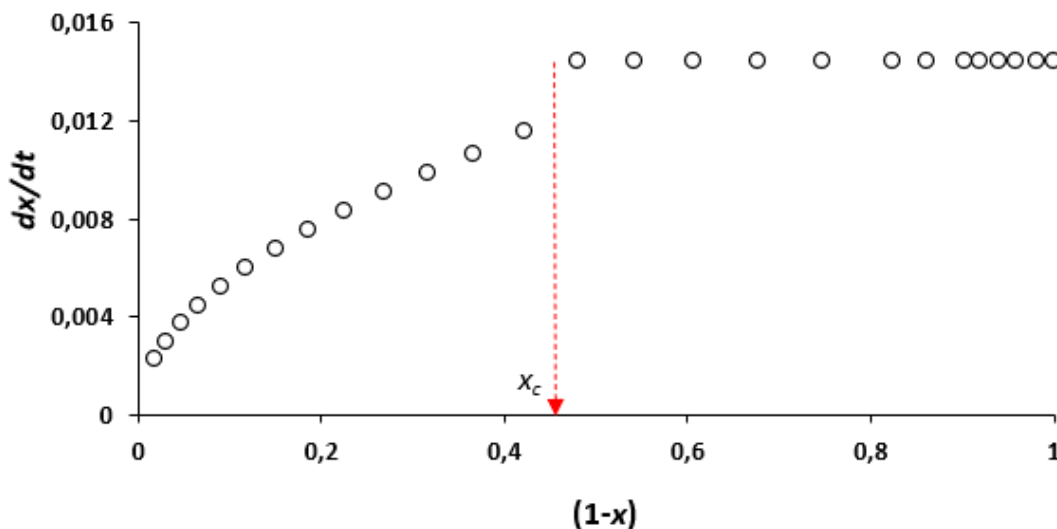


Figure 2. Krischer curve at 50 °C and 87 kPa for the drying of a compost made from coffee dregs.

The initial constant-rate kinetic phase is clearly observed, up to the critical drying degree x_c . After x_c is achieved, the system obeys a first-order rate law, which is $dx/dt = k_1 (1 - x)$. For the experiment shown in figure 2, the linear relationship between dx/dt and $(1 - x)$ is observed in the range from $(1 - x) = 0,423$ to $(1 - x) = 0,151$. We commonly accept a r_p value of $\sim 0,999$ to define the first-order kinetic phase. The k_1 is obviously the slope in the linear range, calculated by least-squares fitting.

The first-order rate constant is found to depend directly on the mean particle-surface/air area. Therefore, the useful datum needed to evaluate for this kinetic stage is $k_2 = k_1 /$ fluxional area.

The fluxional area of a particular sample can be calculated from $(-dm/dt)_{initial}$ and the rate of evaporation of H_2O at the working temperature [e. g. $r_{evap}(H_2O, 50\text{ °C}) = 0,18\text{ g s}^{-1}\text{ m}^{-2}$ at 50 °C], according to the following relation:

$$\text{Fluxional area} = \frac{(-dm/dt)_{initial}\text{ g s}^{-1}}{r_{evap}(H_2O)\text{ g s}^{-1}\text{ m}^{-2}} \quad (5)$$

k_2 values can be used to compare the internal diffusion ability of fluids imbibing porous materials (*vide infra*).



It is possible sometimes to observe a third kinetic phase, depending on the precision of the $m(t)$ values as the final stage of the drying process occurs. If this third stage takes place driven by concentration gradients in the pore system, the advance of the drying process occurs as a function of $t^{1/2}$ as expected from compliance to Fick's second law, though fitting of experimental results to analytical integration of the diffusion equation have become a more common procedure (Carter and Kibler, 1978; Mora, et al., 2019). When capillary forces are at work, the easiest way to quantify the process is by empirically fitting the $x(t)$ data to a power law, t^q ($q \neq 1/2$).

Despite the natural heterogeneity of lignocellulose material samples, the reproducibility of kinetic drying parameters such as $(dx/dt)_{\text{initial}}$, x_c and k_2 can be obtained with mean uncertainties of the order of 8 %, 11 % and 11 %, respectively. The latter mass data shown in figure 1 (third kinetic phase) give $x/m_{\text{final}} = (2,4 \pm 0,7) \text{ g}^{-1} t^{(0,43 \pm 0,02)}$, a result with an associated 30 % uncertainty, calculated as standard deviation. The uncertainties associated to this last rate parameter are larger than for those of the earlier kinetic phases, due to fewer data points and their lesser accuracy.

Calculation of the pseudo first-order rate constant

The calculation of accurate dx/dt values is important, and a derivable function of x in terms of time is needed. This is done empirically, and Occam's razor is the most prudent way to follow. The mass–time data pairs after x_c are fitted to a cubic polynomial, for the direct calculation of dx/dt . The cubic choice is based on the need of having enough curvature ($d^2m/dt^2 \neq 0$) for the calculation of $-dm/dt$ at the various times. The use of higher-degree polynomials should be avoided, because over smoothing of the $m(t)$ data may lead to concealing or distortion of physical information, and substantial errors may result in the further design of an industrial dryer (Kemp, 2001). Two curves may be close together, but still have different slopes (Scheid, 1968).

In any case, it is important to bear in mind that the polynomial fitting has no physical meaning, since it is just a regression equation. The fitting can be obtained by using *Excel* or any suitable software:

$$x(t) = a + bt + ct^2 + et^3 \quad (6)$$

The values of dx/dt at different times come from direct differentiation and evaluation at the various times:

$$\frac{dx}{dt} = b + 2ct + 3et^2 \quad (7)$$

Discussion

A. Follow up from raw biomaterial to final product

It is important to evaluate how different the physical structures of raw biomaterials and final products result, after a certain process is performed. For the mentioned H₂O-soaked compost made from coffee dregs and the original raw agro-industrial residue [(82,7 ± 0,2) % H₂O content], one obtains the following kinetic parameters at 50 °C as shown in Table 1:

Table 1. Effect of composting on the drying kinetic features of coffee dregs, 50 °C and 87 kPa.

Parameter	Raw coffee dregs	H ₂ O-soaked compost
% (H ₂ O) _{desorbed, 50 °C}	77 ± 5	42 ± 1
10 ⁴ (dx/dt) _{initial} / s ⁻¹	3,4 ± 0,8	2,6 ± 0,1
X _c	0,50 ± 0,05	0,50 ± 0,02
10 ² k ₂ / s ⁻¹ m ⁻²	2,5 ± 0,4	5,65 ± 0,07

a) The amount of H₂O desorbed from the initial raw material is greater than the case of final H₂O-soaked compost [(77 ± 5) % vs. (42 ± 1) %, $p < 0,01$). The datum for the raw dregs sample is the sum of “surface”, intra-matrix, and inter-particle H₂O. The experiment with the dregs was done without pressing the sample between kitchen towels, as described above.

b) The initial relative rates of drying [(dx/dt)_{initial}] showed no statistically significant variation. It is known that the rate of evaporation of liquids is independent of the



surface the fluid lays down (Geankoplis, 2006), being only dependent on the geometrical features of particles that define the magnitude of the fluxional area. Comparison of the x_c values cannot be done from these results, because the elimination of the excess inter-particle H_2O was not effectuated for the case of the raw dregs sample.

c) A significant difference was observed in the values of the mass-transfer parameter [k_2]. The result is understood by keeping in mind that composting changes the chemical and physical structure of materials, and consequently, the dynamic porosity of the initial substrate becomes altered. One can believe the 2,3 X difference in k_2 between the final compost product and the initial dregs material is the result of lower tortuosity of pores resulting from the composting process.

B. Comparison of dynamic porosity of different lignocellulosic biomasses

A study discussed by Puente-Urbina et al. (2016) is a good example of the usefulness of the simple procedure presented in this article.

The potential value of forest and agro-industrial residues as solid fuels is well appreciated by the agribusiness sector. The materials must have low moisture content, and the ease of drying of these raw feeds is a central point for the assessment of lignocellulosic stuffs as thermal energy assets. Because drying is an energy-demanding unit operation, the molecular aspects of water diffusion in biomass pores are important to consider for their utilisation as fuels. Diffusion of fluids in pores is also significant for the understanding of combustion and other thermochemical conversions, such as gasification and pyrolysis. Flames originate from the oxidation of the thermally produced gases, that “catch fire” once in contact with oxygen at the particles’ surfaces. Incomplete combustion gives rise to undesired amounts of carbon monoxide, hydrocarbons and tar. This results in lower combustion power and high emission of pollutants.

Puente-Urbina, et al. (2016) determined the x_c of 14 sawdust samples of tropical trees of commercial and environmental importance: *Carapa guianensis*, *Vochysia guatemalensis*, *Lecythis ampla*, *Tectona grandis* L. f., *Enterolobium cyclocarpum*, *Gmelina arborea*, *Cordia*



alliodora, *Ficus werkleana*, *Cedrela odorata* (orange tint), *Cedrela odorata* (dark tint), *Pinus caribaea*, *Samanea saman*, *Rollinia* sp., *Hyeronima alchorneoides*.

Thirteen (13) species showed an average $x_c = 0,26 \pm 0,03$ whereas *L. ampla* showed the higher value $x_c = 0,41 \pm 0,02$. The results can be kinetically interpreted as the latter having a greater degree of dynamic porosity. The authors discussed that *L. ampla* may have been considered different from the beginning, because this species' sapwood has more vascular fibres. Its fresh wood is heavy (high degree of compaction) with specific gravity of about 0,60 – 0,90 in the dry state, compared to the average value $0,4 \pm 0,1$ in the group of reference ($p < 0,01$). From the anatomical viewpoint, it can be said that high specific gravities correlate with thicker xylem walls (higher mass-transfer capacity).

C. Drying of fresh wood

The incorporation of agro-industrial and forestry residues in the production of construction particle boards is an option to minimise the polluting effect of this kind of residuary materials. Agro-industrial remnants are also of value as animal food, animal bedding, or generation of process-heat and steam. Their ashes can be used as source of minerals to produce fertilisers and incorporated into circular-economy opportunities. Whatever final use they are aimed at, they require easy handling and storage stability, and the least possible moisture content.

Drying is an energy-demanding unit operation, and therefore it is necessary to consider the dynamic porosity of the materials whose water content must be reduced. The minimum energy expenditure in laboratory conditions of a porous material can be estimated from its drying curve.

The residential electric outlet in Costa Rica gives 110 V electric potential, and the balances in our laboratory consume 4 A electric current. For a particular test, the normalised electrical energy used by the drying balances equals to the quantity $(110 \text{ V} \times 4 \text{ A} \times \text{time})/m_{\text{initial}}$ (Puente-Urbina, et al. 2016; Conejo-Barboza and Mata-Segreda, 2018). A plot of energy vs. amount of residual moisture can be constructed, and figure 3 shows the case of the drying of a sample of the compost mentioned above as example.

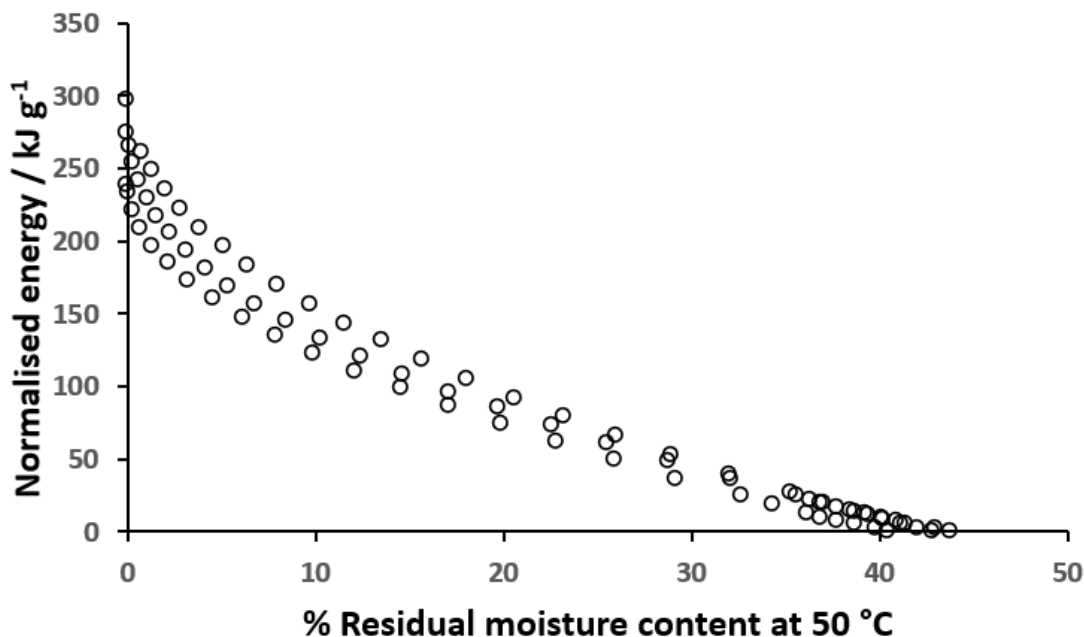


Figure 3. Laboratory normalised energy cost for the drying of H₂O-soaked compost from coffee dregs, 50 °C, 87 kPa and laboratory relative humidity ~ 65 %.

A linear relationship between the energy used and the amount of residual moisture can be observed in the range from the initial condition down to ~21 % of residual moisture content. This limit corresponds to $x_c = 0,50 \pm 0,05$. The molecular mechanism of this drying stage corresponds to “superficial” evaporation, as the rate determining step; a situation like the evaporation from a free-liquid surface. Beyond this point, drying depends on internal diffusion through the solid matrix pores. Since now there is less drying (H₂O evaporation) per unit thermal energy input, the process deviates from the initial linearity. Botanists and plant physiologists may find this kind of observation of interest to establish structure-function correlations.

Engineers may be able to estimate the minimal amount of thermal energy needed to conduct the drying process of porous materials, by interpolation from plots such as the one shown. The actual energy cost is obviously dependent on the nature of the material to be dried, the amount of raw material, its degree of hydration, desired final moisture content,



heating input, mechano-electrical energy needed for forced purging air currents, heat sinks, etc.

Conclusion

The proposed methodology is simple to conduct, and allows the microscopic understanding of processing, either theoretically based or by trial and error, in terms of the supramolecular idiosyncrasies of the porous materials to be dried.

Both x_c and k_2 kinetic parameters can be used to assess diffusional barriers in porous matrices, allowing comparison amongst materials. x_c is easier to determine, and one reckons that it is by itself enough to make comparisons of mass-transfer resistance between different porous materials.

References

- Alcántara, C.M., Moreira, I.d.S., Cavalcanti, M.T., Lima, R.P., Moura, H.V., da Silva Neves, R., Cassimiro, C.A.L., Martins, J.J.A., da Costa Batista, F.R., Pereira, E.M. (2024). Mathematical modelling of drying kinetics and technological and chemical properties of *Pereskia* sp. Leaf Powders. *Processes*, 12, (10), 2077. <https://doi.org/10.3390/pr12102077>.
- Cai, J., Zhu, L., Wei, Q., Huang, D., Luo, M., Tang, X. (2023). Drying kinetics of a single biomass particle using Fick's second law of diffusion. *Processes*, 11(4), 984. <https://doi.org/10.3390/pr11040984>.
- Carter, H. G., Kibler, K. G. (1978). Langmuir-type model for anomalous moisture diffusion in composite resins. *Journal of Composite Materials*, 12(2), 118-131. <https://doi.org/10.1177/002199837801200201>.
- Conejo-Barboza, G., & Mata-Segreda, J. F. (2018). Drying kinetics as tool for the assessment of dynamic porosity of catalyst-support materials. *International Journal of Renewable Energy & Biofuels*, article ID 901967, [Doi: 10.5171/2018.901967](https://doi.org/10.5171/2018.901967).
- Fernández-Solano, B. & Mata-Segreda, J. F. (2021). Effect of molecular structure on diffusion of alcohols through type-A zeolite pores (0.5 nm). *Journal of Materials Science and Engineering A*, 11(4–6), 48-55. <https://doi.org/10.17265/2161-6213/2021.4-6.003>
- Geankoplis, C. J. (2006). *Procesos de transporte y principios de procesos de separación*. (4.ª ed. en español). Compañía Editorial Continental, pp. 589-594.
- Inyang, U. E., Oboh, I.O., & Etuk, B. R. (2018). Kinetic models for drying techniques – Food materials. *Advances in Chemical Engineering & Science*, 8 (2), 27-48. <https://doi.org/10.4236/aces.2018.82003>.
- Kemp, I. C., Fyhr, B. C., Laurent, S., Roques, M. A., Groenewold, C. E., Tsotsas, E., Sereno, A. A., Bonazzi, C. B., Bimbenet, J.-J., and Kind, M. (2001). Methods for processing experimental drying kinetics data. *Drying technology*, 19(1), 15-34.



<https://doi.org/10.1081/DRT-100001350>.

Mata-Segreda, J. F. (2025). Evaporation kinetics of household and industrial liquids as an index for safe handling and storage. *ACS Chemical Health & Safety*, 32(2), 115-121.

<https://doi.org/10.1021/acs.chas.4c00091>.

Mora, E., González, G., Romero, P., Castellón, E. (2019). Control of water absorption in concrete materials by modification with hybrid hydrophobic silica particles. *Construction & Building Materials*, 221, 210-218. <https://doi.org/10.1016/j.conbuildmat.2019.06.086>.

Puente-Urbina, A., Morales-Aymerich, J. P., Kim, Y. S., & Mata-Segreda, J. F. (2016). Drying kinetics and assessment of relative energy cost for drying of woody biomasses. *International Journal of Renewable Energy & Biofuels*, article ID 701233, <https://doi.org/10.5171/2016.701233>

Schlaich, A., Barrat, J.-L., Coasne, B. (2025). Theory and modelling of transport for simple fluids in nanoporous materials: From microscopic to coarse-grained descriptions. *Chemical Reviews*, 125 (5), 2561-2624. <https://doi.org/10.1021/acs.chemrev.4c00406>

Scheid, F. (1968) *Numerical analysis*. McGraw-Hill, New York, chapter 13.

Smirnov, M. S., & Lysenko, V.I. (1989). Equations of drying curves. *International Journal of Heat and Mass Transfer*, 32 (5), 837-841. [https://doi.org/10.1016/0017-9310\(89\)90232-9](https://doi.org/10.1016/0017-9310(89)90232-9).

Songgok, J., Bousfield, D., Ridway, C., Gane, P., Toivakka, M. (2012). Drying of porous coating: Influence of Coating Composition. *Industrial & Engineering Chemistry Research*, 51(42), 13680-13685. <https://doi.org/10.1021/ie301624e>

Yiotis, A. G., Tsimpanogiannis, I. N., Stubos, A. K., & Yortsos, Y. C. (2006). Pore-network study of the characteristic periods in the drying of porous materials. *Journal of Colloid and Interface Science*, 297(2), 738-748. <https://doi.org/10.1016/j.jcis.2005.11.043>